Simulation of Single-Channel Optical Systems at 100 Gb/s

Dietrich Marcuse, *Life Fellow, IEEE,* and Curtis R. Menyuk, *Fellow, IEEE*

***Abstract*— With the help of a computer simulation, we have investigated the conditions under which the transmission of light pulses through optical fibers may be possible over thousands of kilometers at a bit rate of 100 Gb/s. Employing an amplifier spacing of only 20 km, nonreturn-to-zero (NRZ), return-to-zero (RZ), and dispersion-managed solitons (DMS's) may all be useful provided that certain additional conditions are met. These include dispersion management by means of a dispersion map, a reduced dispersio**
n slope, low polarization mode dispersion (PMD), and in-line optical filters.

***Index Terms*— High-speed communication, optical communication, optical fibers, optical fiber communication, optical fiber theory, nonlinear optics, nonlinear wave propagation.**

I. Introduction

DESPITE the great success of wavelength division multiplexed (WDM) systems in achieving high-capacity transmission, there remains interest in exploring the capabilities of high data rate, single-channel systems for at least specialized applications. In this communication we investigate by means of computer simulations the possibility of transmitting a single channel at 100 Gb/s over 500 km or more. The length of 500 km would be sufficient, for example, to connect many of the major government laboratories in the Washington, DC area. Point-to-point links using a return to zero (RZ) pulse format have been studied by Saruwatari and his colleagues in a series of ground-breaking experiments [1]. Typical propagation lengths were 200 km. The key difficulties that they encountered were finding effective methods for clock recovery and demultiplexing. Techniques for resolving these issues are compared in detail in [1]. In the last few years, there has been considerable interest in finding network designs that take advantage of the existing techniques, and considerable progress has been made [2], [3]. Moreover, there has been continued progress in developing the optical components needed for these networks such as optical memories [4]. The task of developing the optical components needed for operation at 100 Gb/s and determining network architectures that can operate successfully with these components are so daunting that the task of optimizing the optical fiber transmission line itself to achieve the maximum possible distance has received relatively short shrift. In much of the work to date, it has been assumed that these high-speed, single-channel networks would be based on standard soliton transmission [2], [3], but the use of standard solitons limits the transmission length to around 100 km [3].

In this communication, we show that by using both relatively short amplifier spacings and dispersion maps—both are 20 km—it is possible to transmit signals as much as 2000 km with acceptable eye openings. The key point in lowering the amplifier spacing is that it allows us to lower the accumulation of amplified spontaneous emission (ASE) noise. The rate at which noise accumulates is proportional to $[\exp(\alpha L_{\rm amp})-1]/L_{\rm amp}$, where α is the fiber attenuation rate and $L_{\rm amp}$ is the amplifier spacing. By reducing the amplifier spacing from 80 km, which is common in current terrestrial systems, to 20 km, we reduce the rate of noise accumulation by a factor of 6. Depending on the signal format and the distance we propagate, we are then able to achieve acceptable eye diagrams with peak powers comparable to those in current systems. The key point in lowering the map period at 100 Gb/s is that with the larger bandwidth of the channel, the periodic or nearly periodic oscillations in the dispersion map are large enough to disrupt the four-wave mixing but are not so large that they lead to excessive intersymbol interference between the bits.

We studied nonreturn-to-zero (NRZ), return-to-zero (RZ), and dispersion-managed soliton (DMS) propagation. The NRZ pulses are generated as perfect rectangular shapes with time slots of length T. These pulses are rounded by filtering with a Bessel filter of order four and baseband bandwidth, $B = 85$ GHz. The RZ pulses used in this simulation have the following raised cosine shape which is also impressed on the field envelope:

$$f = \frac{1}{2}\left[1 - \cos\left(\frac{2\pi}{T}t\right)\right], \qquad \text{for } 0 \le t \le T. \tag{1}$$

The pulses are launched without an initial chirp. While there is evidence that an initial phase modulation can lead to an improved performance in wavelength division multiplexed systems [5], we did not find it necessary in our system. The DMS pulses are launched as Gaussian waveforms of the envelope of the optical field (not its intensity) whose optimal width can be computed from the theory in [6]. DMS pulses have numerous advantages over standard solitons as discussed, for example, in [7]. In the context of 100 GB/s transmission a particular advantage is that the DMS pulses have significantly

Manuscript received May 13, 1998; revised December 28, 1998. This work was supported by grants from the AFOSR, NSF, and DOE.

The authors are with the Department of Computer Science and Electrical Engineering, University of Maryland Baltimore County, Baltimore, MD 21250 USA.

Publisher Item Identifier S 0733-8724(99)02695-X.

lower peak powers than standard solitons and are thus not affected by the Raman effect. The Raman effect can seriously degrade soliton performance at high data rates [8].

In this communication, we consider prototypical RZ, NRZ, and DMS pulses because all three pulse forms have been the subject of recent experimental and theoretical studies, and we determine their tolerances to variations of the dispersion, power, polarization mode dispersion (PMD), and dispersion slope. However, note that there is no fundamental distinction between the different formats. When we raise the power of an RZ pulse, it tends to contract as it propagates and can eventually look like a DMS pulse; conversely, when we lower the power of a DMS pulse, it tends to spread as it propagates and can eventually look like an RZ pulse. In our simulations, the NRZ pulses had no initial phase modulation and did not transform into RZ pulses, but work by others [5] shows that this is possible.

Successful signal transmission at 100 Gb/s requires that several additional conditions are met. To be able to reach distances of several thousand kilometers, even with DMS, requires a low dispersion slope in addition to a carefully designed dispersion map. We find that a few thousand kilometers can be bridged with $dD/d\lambda = 0.03$ ps/(nm^2-km). Pulse transmission over long distances is also helped by using in-line filters [12]. Finally, PMD must be kept low and the signal power must be held within certain ranges which depend on the chosen modulation format and become narrower as the transmission distance is increased.

We also looked at the influence of the Raman nonlinearity and found that its contribution to our calculations did not alter the results significantly. Therefore, it was not included in the discussions presented in this paper.

II. Scaling Laws

Transmitting light pulses through fibers becomes increasingly more difficult as the bit rate increases. This fundamental property can be seen by inspection of the coupled nonlinear Schrödinger equation which governs light transmission through very long optical fibers incorporating the influence of dispersion, PMD, and the Kerr nonlinearity of the fiber [13], [14]

$$i\frac{\partial \mathbf{U}}{\partial z} + (\sigma_3 \cos\theta + \sigma_1 \sin\theta)\left(\Delta\beta \mathbf{U} + i\frac{d(\Delta\beta)}{d\omega}\frac{\partial \mathbf{U}}{\partial t}\right) - \frac{1}{2}\left(\frac{d^2\beta}{d\omega^2}\right)\frac{\partial^2 \mathbf{U}}{\partial t^2} - \frac{i}{6}\left(\frac{d^3\beta}{d\omega^3}\right)\frac{\partial^3 \mathbf{U}}{\partial t^3} + \gamma\left[|\mathbf{U}|^2\mathbf{U} - \tfrac{1}{3}(\mathbf{U}^\dagger\sigma_2\mathbf{U})\sigma_2\mathbf{U}\right] = 0. \quad (2)$$

The z-coordinate measures the actual length along the fiber while t refers to the retarded time measured relative to the moving pulse, ω represents the angular frequency of the carrier wave which travels with the propagation constant β. The constant γ is defined as $\gamma = n_2\omega/cA_{\text{eff}}$ where n_2 is the nonlinear coefficient of the fiber, c is the velocity of light in vacuum, and A_{eff} is the effective area of the guided fiber mode. The field $\mathbf{U}$ is a two-dimensional vector whose components represent the envelope of the two polarization components of the electric field of the light wave. The vector is normalized so that $|\mathbf{U}|^2$ represents the power carried by the guided wave. The argument θ of the sine and cosine functions equals twice the angle defining the orientation of the fiber's birefringence axis relative to a fixed coordinate system. The Pauli σ-matrices are defined as

$$\sigma_1 = \begin{pmatrix} 0 & 1 \\ 1 & 0 \end{pmatrix}, \quad \sigma_2 = \begin{pmatrix} 0 & -i \\ i & 0 \end{pmatrix}, \quad \sigma_3 = \begin{pmatrix} 1 & 0 \\ 0 & -1 \end{pmatrix}. \quad (3)$$

By inspection of the coupled nonlinear Schrödinger equation it is easy to see that the following scale transformation leaves its solutions invariant:

$$t' = \kappa t, \quad z' = \kappa z, \quad \left(\frac{\partial^2\beta}{\partial\omega^2}\right)' = \kappa\frac{\partial^2\beta}{\partial\omega^2}, \quad \left(\frac{\partial^3\beta}{\partial\omega^3}\right)' = \kappa^2\frac{\partial^3\beta}{\partial\omega^3}, \quad |U'|^2 = \frac{1}{\kappa}|U|^2. \quad (4)$$

The scaling parameter, κ, connects the original variables with the transformed quantities that are marked with primes. Since the nonlinear Schrödinger equation deals with the field envelope instead of the field itself, the scale transformation affects only the scale of the overall temporal and spatial pulse width but not the carrier frequency or the wavelength of the optical field. Thus, the wavelength λ and the angular frequency ω are not affected by it.

This scale transformation reveals a number of interesting properties. If we want to scale a system from operation at 10 to 100 Gb/s, we have $\kappa = 0.1$. Thus, if the 10 Gb/s system begins to experience transmission difficulties at 10 000 km, the 100 Gb/s system can bridge a distance of only 1000 km. Simultaneously, the period length of the dispersion map as well as the dispersion values, $d^2\beta/d\omega^2$, must also be reduced by a factor of 10 while the peak power of the pulses must be increased by a factor of 10. Particularly troublesome is the dispersion slope, $d^3\beta/d\omega^3$. If a certain slope value could be tolerated at 10 Gb/s, at 100 Gb/s the acceptable value of the dispersion slope is 100 times smaller!

The value of the difference $\Delta\tau$ in arrival time of pulses polarized in the two principal polarization states is not affected by the scale transformation (4). This time difference is the cause of PMD [15], [16]. However, of more practical interest is the fiber length scale L_{PMD} over which a signal pulse with bandwidth $\Delta\nu$ suffers an average temporal width increase $\langle|\Delta\tau|\rangle$. From the relationship $\langle|\Delta\tau|\rangle = D_{\text{PMD}}\sqrt{L_{\text{PMD}}}$ and the fact that the permissible temporal spread is inversely proportional to the signal bandwidth, we have $L_{\text{PMD}} = 1/D_{\text{PMD}}^2(\Delta\nu)^2$. Therefore, the length scale is proportional to $(\Delta\nu)^{-2}$. Since $\Delta\nu$ is proportional to $1/\kappa$, it follows that $L_{\text{PMD}} \propto \kappa^2$. We thus find once again that the acceptable value of D_{PMD} for a fixed propagation length is reduced by a factor 10 when scaling from 10 to 100 Gb/s.

III. System Parameters

Our simulation of the transmission is characterized by a large number of different parameters, most of which did not change from simulation to simulation. For completeness, we

list a typical parameter set below, and mention deviations from these values whenever they occur.

- bit rate: 100 Gb/s or $T = 10$ ps;
- number of bits per word: 64;
- wavelength: $\lambda = 1.55$ μm;
- amplifier spacing: $L_{\text{amp}} = 20$ km;
- excess noise factor of amplifier: $n_{\text{sp}} = 1.5$;
- effective mode area: 55 μm^2;
- polarization beat length: 50 m;
- fiber correlation length: 100 m;
- polarization mode dispersion: $D_{\text{PMD}} = 0$;
- dispersion map with $\langle D \rangle = 0$
  - period length: 20 km;
  - first leg: 5 km, $D = 0.3$ ps/(nm-km);
  - second leg: 10 km, $D = -0.3$ ps/(nm-km);
  - third leg: 5 km, $D = 0.3$ ps/(nm-km);
- dispersion slope: $dD/d\lambda = 0.03$ ps/(nm^2-km);
- fiber power loss: $\alpha = 0.2$ dB/km;
- nonlinear coefficient: $n_2 = 2.6 \times 10^{-16}$ cm^2/W;
- optical in-line Bessel filters:
  - spacing: 20 km;
  - bandwidth: 500 GHz for DMS; 1200 GHz for NRZ and RZ;
  - order number: 4;
- electrical Bessel filter:
  - bandwidth: 85 GHz;
  - order number: 5.

The full-width at half maximum (FWHM) of the Gaussian DMS pulses was 2.56 ps while the FWHM of the RZ pulses is 0.364 $T = 3.64$ ps according to (1). In this simulation, the amplifiers were modeled as multipliers with a flat frequency response that do no more than compensate for the fiber loss. However, at each amplifier the appropriate amount of random Gaussian noise is added to each component of the Fourier spectrum of the optical signal.

The in-line filters were given a different bandwidth for DMS and NRZ as well as RZ modulation because the DMS spectrum remains more or less constant along the fiber while the spectra of the NRZ and RZ signals become increasingly wider by self-phase modulation, so that it was considered necessary to provide them with a wider spectral range to grow into. The final so-called electrical filter operates at baseband and filters the square magnitude of the signal.

IV. Tolerances to Variations of the Peak Pulse Power

Ideally, an assessment of the satisfactory operation of the system should be based on bit error rates. However, this figure of merit is notoriously difficult to estimate from computer simulations. Closely related to the bit error rate is another figure of merit, the Q-factor, which is defined as the difference between the average levels of the pulses and spaces divided by the sum of their standard deviations. However, the relation between Q and the bit error rate exists only if the spread of the levels is caused entirely by noise. In most real systems, as well as in our simulation, the spreading of the pulse and space levels is caused substantially by intersymbol interference so that a Q-factor computed according the above definition would have no easily definable relation to the bit error rate. For this reason, we use as our criterion for "acceptable" system operation the ratio of the eye opening to the average level of the top rail (pulse level) of the eye.

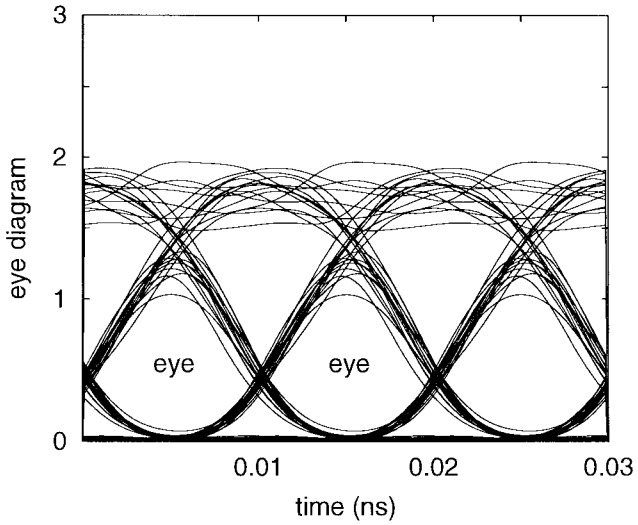

Fig. 1. An eye diagram for NRZ-pulses which was judged to be acceptable. The ratio of the eye opening to the average level of the upper rail of the eye is 0.57.

For illustrative purposes, a "good" and a "just acceptable" eye diagram are shown for NRZ pulses in Figs. 1 and 2. An eye diagram was deemed acceptable when the ratio of the eye opening to the average height of the top rail of the eye was larger than 0.3. In Fig. 1 this ratio is 0.57 while it is only 0.33 in Fig. 2. As can be seen in Fig. 2, it is often not immediately obvious which part of the diagram represents the eye opening. Since there are as many pulses as there are spaces in our 64 bit word pattern, there must be 32 lines above and 32 below the opening. Therefore, we identify the smaller areas labeled "eye" as the true openings and not the larger open areas at a slightly higher level.

We consider systems of 500, 1000, 1500, and 2000 km in length. In the case of DMS modulation, the middle section of the dispersion map was set at $D = -0.25$ ps/(nm-km) so that the average anomalous dispersion of one period of the dispersion map was $\langle D \rangle = 0.025$ ps/(nm-km).

The dependence of the system performance on the path-averaged peak power of the launched pulses is summarized in Fig. 3. Path averaging is used since analytical solutions of the nonlinear Schrödinger equation are usually given for lossless fibers. In a real system, fiber loss is compensated by periodically placed optical amplifiers so that the pulse power falls and rises due to the interplay of loss and amplification. For many purposes, a path average of the pulse power can serve as a good approximation to the fixed power levels of a lossless system. By definition, the relation between path-averaged power, P_{av}, to pulse peak power, P_{o}, at the fiber input (launched power) is given by

$$P_{\text{av}} = \frac{1 - \exp(-\alpha L_{\text{amp}})}{\alpha L_{\text{amp}}} P_{\text{o}}. \tag{5}$$

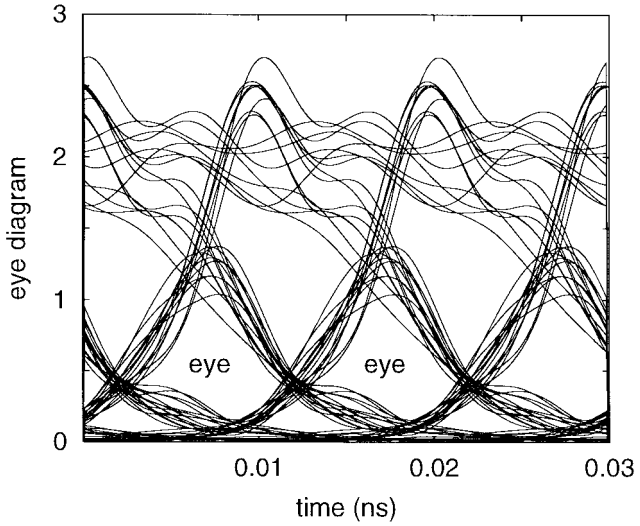

Fig. 2. An eye diagram for NRZ-pulses which was judged to be barely acceptable. The ratio of the eye opening to the average level of the upper rail of the eye is 0.33.

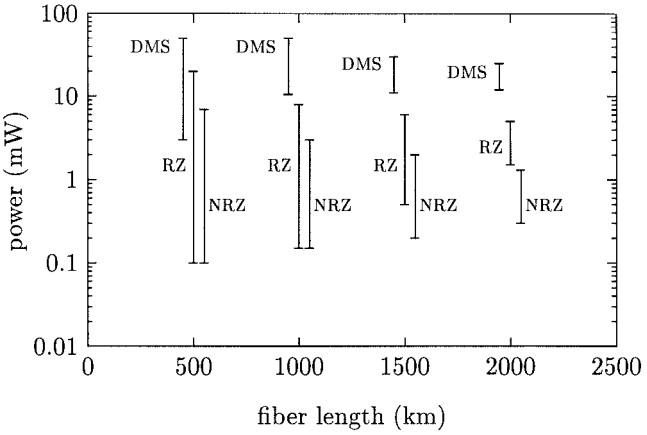

Fig. 3. Tolerance of the 100 Gb/s systems to path-averaged peak pulse power variations. Note that the entries for DMS and NRZ are displaced from their positions at 500, 1000, 1500, and 2000 km for clarity of presentation.

The vertical lines clustering at fiber lengths of 500, 1000, 1500, and 2000 km describe DMS-, RZ-, and NRZ-systems at these lengths. The positions of the lines representing DMS- and NRZ-systems have been displaced sidewise to avoid overlap. The end points of the vertical lines delineate the lowest and highest (path-averaged) peak pulse powers that were judged to be acceptable for reliable performance of the systems at the indicated fiber lengths. Throughout most of this work, the path-averaged peak pulse power of RZ and NRZ pulses at the fiber input, and after each subsequent amplifier, is held at 1 mW. However, it can be seen in Fig. 3 that RZ pulses would not be viable at a distance of 2000 km if the signal level were held at 1 mW. However, since Fig. 3 represents the results of investigating the system tolerance to power variations, the RZ pulse modulation format is listed at the 2000 km length since it becomes viable in a power range between 1.5 and 5 mW. The RZ pulses do not work at higher power levels because of our insistence that pulses are regarded as being of the RZ type if the average dispersion vanishes. At small positive values of the

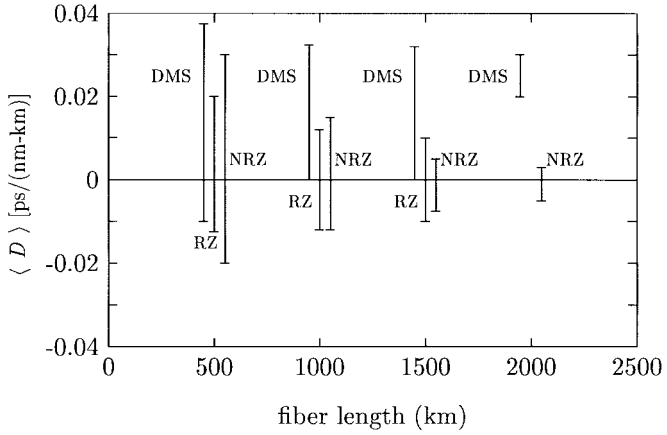

Fig. 4. Tolerance of the 100 Gb/s systems to variations of the average dispersion.

average dispersion, RZ pulses would perform better at higher power levels and would become indistinguishable from DMS pulses. Likewise, DMS pulses could operate at higher power levels if the average dispersion were raised above $\langle D \rangle = 0.025$ ps/(nm-km). As mentioned in the introduction, there is no fundamental distinction between RZ and DMS modulation formats. At 2000 km, the NRZ-system works marginally at the 1 mW average peak power level. Of the three modulation formats, NRZ can operate with the lowest peak power.

V. Tolerances to Variations of the Average Dispersion

The tolerance of the system to variations of the average dispersion is shown in Fig. 4. The average dispersion was changed by changing the normal dispersion value of the middle section of the dispersion map. The vertical lines indicate once more the lower and upper limits of the permissible average dispersion for each modulation format. It is important to note that the dispersion tolerances were computed for 14 mW path-averaged peak power for DMS pulses and 1 mW path-averaged peak power for RZ and NRZ pulses. An increase of the power of the RZ pulses would improve the performance substantially since at higher power levels RZ pulses behave like DMS pulses. However, this comment does not apply to NRZ pulses. Raising their power does not result in DMS behavior but may make the system inoperable. The tendency for this can be seen in Fig. 3 where the upper power limits for NRZ pulses lie consistently below those of RZ pulses. Under the stated conditions, the NRZ-system does not operate well and the RZ-system not at all at $L = 2000$ km; therefore, RZ-pulses are not shown at this length in Fig. 4.

VI. Tolerance to PMD

PMD can cause significant degradation of system performance. As a random variable with a wide (Maxwellian [17]) distribution, the actual value of D_{PMD} depends on the particular distribution of the randomly varying birefringence along the fiber. In our simulation, the actual values of the difference of the group delays of the two principal states of polarization depend at any given frequency on the choice

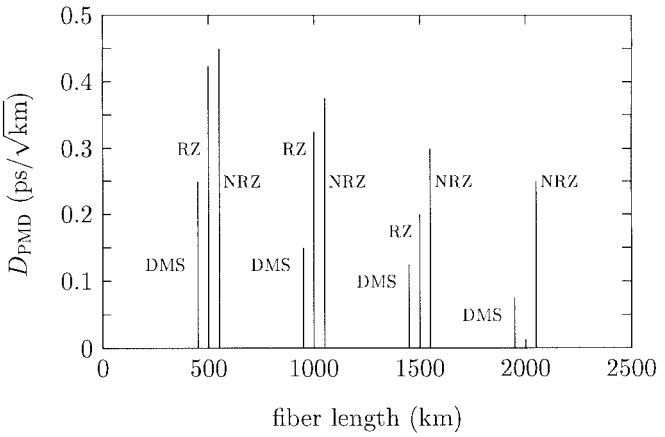

Fig. 5. Tolerance of the 100 Gb/s system to PMD. The short line at 2000 km is not an indication of RZ pulses but a tic mark.

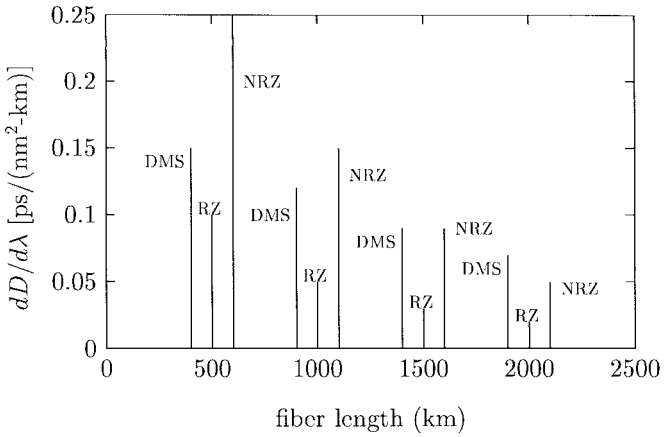

Fig. 6. Tolerance of the 100 Gb/s system to the dispersion slope.

of random variables used to construct the birefringent fiber. However, at the high bit rate considered in this paper, the signal spectrum is so wide that there is little correlation among the polarization group delays of widely separated spectral components. For this reason, it was found that changing the seed of the random number generator for producing the fiber statistics has only a small effect on the observed signal distortion.

Fig. 5 shows the ranges of the permissible PMD values for each of the three modulation formats at 500, 1000, 1500, and 2000 km fiber length. The PMD tolerance study uses again the path-averaged peak power levels mentioned in the last section. It is of interest to observe that the permissible PMD range is smallest for DMS, the modulation with the widest signal spectrum. It is somewhat wider for RZ with a somewhat narrower spectral range and it is widest for NRZ with the narrowest spectral range. This is another indication of the rapid variation of the principal state as a function of frequency. At 2000 km, RZ pulses are not listed since they are not viable at this distance at the 1 mW power level. The short line seen at 2000 km is a tic mark.

VII. Tolerance to the Dispersion Slope

An important fiber parameter is the dispersion slope, $dD/d\lambda$. So far, we have assumed in all our discussions that this parameter has the value $Dd/d\lambda = 0.03$ ps/(nm^2-km). This value was already too large to permit an RZ-system of 1 mW peak power to operate at a fiber length of $L = 2000$ km. A systematic study of the effect of the dispersion slope on system performance is summarized in Fig. 6. The length of the vertical bars indicates the largest value of $dD/d\lambda$ which a system with the indicated modulation format can tolerate at the fiber length specified on the horizontal axis. Once more, we have shifted the value for DMS and NRZ systems sideways to be able to display all three modulation formats on the same graph. However, the average dispersion of the fiber system is not the same for DMS and the other two modulation formats. Following the practice used throughout most of this study, we have again assumed that for the DMS modulation, $\langle D \rangle = 0.03$ ps/(nm-km), while $\langle D \rangle = 0$ was assumed for RZ and NRZ modulation. These average dispersion values are understood to apply at the carrier frequency of the signal. The path-averaged peak power of the DMS pulses is 14 mW and that of the RZ and NRZ pulses is 1 mW.

Interestingly, the RZ modulation is most sensitive to the dispersion slope. However, this observation is contingent on the fact that it is supposed to operate at 1 mW peak power and $\langle D \rangle = 0$. By comparison, NRZ (also at $\langle D \rangle = 0$) proves itself to be surprisingly robust, since at shorter fiber lengths it can tolerate even larger values of the dispersion slope than DMS. This is probably due to the inherently wider temporal width of the NRZ pulses compared with RZ and DMS pulses.

Whereas RZ pulses do not appear at 2000 km in Fig. 5, their appearance in Fig. 6 shows that they are marginally viable at lower dispersion slopes. It must be remembered that in Fig. 5 the dispersion slope was $dD/d\lambda = 0.03$ ps/(nm^2-km).

VIII. Conclusion

We have discussed the possibility of using an optical fiber communications system, operating at a bit rate of 100 Gb/s, at distances of up to 2000 km. The discussion was based on results of computer simulations obtained by numerical solutions of the coupled nonlinear Schrödinger equation by means of the split-step method and included dispersion-managed solitons (DMS), return-to-zero (RZ), and nonreturn-to-zero (NRZ) modulation formats. Our discussion stressed the tolerance limits imposed by fluctuations of the peak pulse power and by deviations from the design values of average dispersion, the polarization mode dispersion, and the dispersion slope. Overall, these tolerance limits appear favorable in the sense that they do not seem to place undue restrictions on the design of such systems. The margins for all three modulation formats are roughly equivalent.

Since our work was aimed at determining the propagation limits in a highly optimized system, we did not do careful studies to determine how the maximum propagation distances degrade as the amplifier spacings increase. However, preliminary work indicates that the maximum propagation distances fall off very rapidly as the amplifier spacing increases beyond 20 km. This topic is an important one for future study.

ACKNOWLEDGMENT

C. R. Menyuk gratefully acknowledges encouragement from Dr. H. Mandelberg and fruitful discussions with Dr. K. Rauschenbach and her co-workers.

REFERENCES

[1] M. Saruwatari, "High-speed optical signal processing for communications systems," *IEICE Trans. Commun.*, vol. E78-B, no. 5, pp. 635–643, 1995.
[2] J. R. Sauer, M. N. Islam, and S. P. Dijaili, "A soliton ring network," *J. Lightwave Technol.*, vol. 11, pp. 2182–2187, Dec. 1993.
[3] R. A. Barry, V. W. S. Chan, K. L. Hall, E. S. Kintzer, J. D. Moores, K. A. Rauschenbach, E. A. Swanson, L. E. Adams, C. R. Doerr, S. G. Finn, H. A. Haus, E. P. Ippen, W. S. Wong, and M. Hanner, "All-optical network consortium—Ultrafast TDM networks," *IEEE J. Select. Areas Commun.*, vol. 14, pp. 999–1013, June 1996.
[4] J. D. Morres, K. L. Hall, S. M. LePage, K. A. Rauschenbach, W. S. Wong, H. A. Haus, and E. P. Ippen, "20-GHz optical storage loop/laser using amplitude modulation, filtering and artificial fast saturable absorption," *IEEE Photon. Technol. Lett.*, vol. 7, pp. 1096–1098, Sept. 1995.
[5] N. S. Bergano and C. R. Davidson, "Wavelength division multiplexing in long-haul transmission systems (Invited Paper)," *J. Lightwave Technol.*, vol. 14, pp. 1299–1308, June 1996.
[6] V. S. Grigoryan, T. Yu, E. A. Golovchenko, C. R. Menyuk, and A. N. Pilipetskii, "Dispersion-managed soliton dynamics," *Opt. Lett.*, vol. 22, pp. 1609–1611, 1997.
[7] N. J. Smith, N. J. Doran, W. Forsiak, and F. M. Knox, "Soliton transmission using periodic dispersion compensation," *J. Lightwave Technol.*, vol. 15, pp. 1808–1822, Oct. 1997.
[8] G. P. Agrawal, *Nonlinear fiber Optics.* San Diego, CA: Academic, 1995, sec. 5.5 and 8.4.
[9] I. Gabitov, E. G. Shapiro, and S. K. Turitsyn, "Optical pulse dynamics in fiber links with dispersion compensation," *Opt. Commun.*, vol. 134, pp. 317–329, 1997.
[10] M. Matsumoto and H. A. Haus, "Stretched-pulse optical fiber communications," *IEEE Photon. Technol. Lett.*, vol. 9, pp. 785–787, 1997.
[11] S. Kumar and A. Hasegawa, "Quasisoliton propagation in dispersion-managed optical fibers," *Opt. Lett.*, vol. 22, pp. 372–374, 1997.
[12] E. A. Golovchenko, J. M. Jacobs, A. N. Pilipetskii, C. R. Menyuk, and G. M. Carter, "Dispersion-managed solitons in a fiber loop with in-line filtering," *Opt. Lett.*, vol. 22, pp. 289–291, 1997.
[13] C. R. Menyuk, "Nonlinear pulse propagation in birefringent optical fibers," *IEEE J. Quantum Electron.*, vol. 23, pp. 174–176, 1987.
[14] ———, "Pulse propagation in an elliptically birefringent Kerr medium," *IEEE J. Quantum Electron.*, vol. 25, pp. 2674–2682, 1989.
[15] C. D. Poole and R. E. Wagner, "Phenomenological approach to polarization dispersion in long single-mode fibers," *Electron. Lett.*, vol. 22, pp. 1029–1030, 1986.
[16] C. D. Poole, N. S. Bergano, R. E. Wagner, and H. J. Schulte, "Polarization dispersion and principal states in a 147-km undersea lightwave cable," *J. Lightwave Technol.*, vol. 6, pp. 1185–1190, 1988.
[17] G. J. Foschini and C. D. Poole, "Statistical theory of polarization dispersion in single mode fibers," *J. Lightwave Technol.*, vol. 9, pp. 1439–1456, 1991.

Dietrich Marcuse (M'58–F'73–LF'95), photograph and biography not available at the time of publication.

Curtis R. Menyuk (SM'88–F'98), photograph and biography not available at the time of publication.